

FIRST OBSERVATIONS OF TERRESTRIAL DUST DEVILS IN ORBITAL IMAGE DATA: COMPARISON WITH DUST DEVILS IN AMAZONIS PLANITIA, MARS. D. Reiss, Institut für Planetologie, Westfälische Wilhelms-Universität, Wilhelm-Klemm-Str. 10, 48149 Münster, Germany.

Introduction: On Mars, dust devils are frequently observed with orbital image data (e.g., 1–5). Terrestrial dust devils have not yet been observed directly in satellite imagery. Here we report about the first terrestrial dust devil observations with visible and thermal satellite data on an alluvial fan in the Taklimakan desert (Fig. 1A). Dust devils were first recognized in high resolution visible image data (Fig. 1B) using Google Earth. Further inspection of medium resolution image data (Aster and Landsat 7 and 8) revealed that dust devils in this area are numerous and large (Fig. 2).

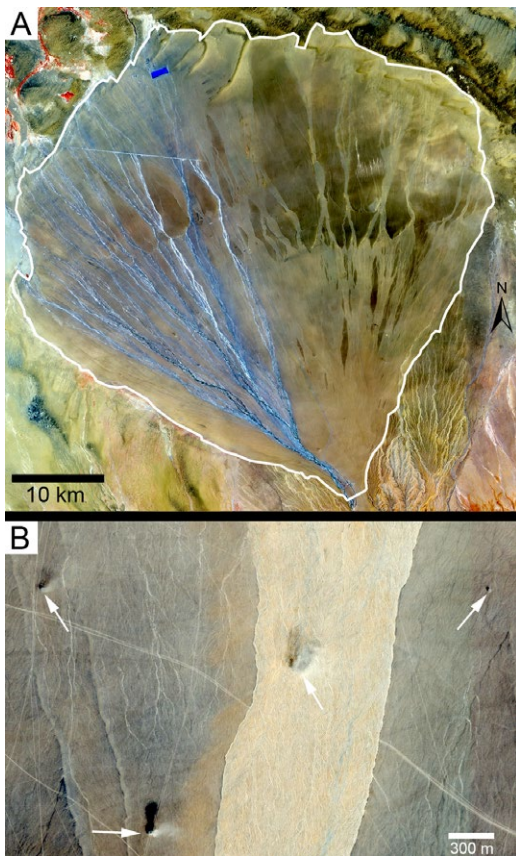


Fig. 1. (A) Alluvial fan at the southern border of the Taklimakan desert (China) at 37.4°N and 84.3°E. White outline shows the study area. Landsat 8 RGB image. (B) High resolution DigitalGlobe image accessed through Google Earth showing 4 dust devils (white arrows) with diameters from left to right of about 15, 30, 75, and 20 m. Also note some faint dark dust devil tracks.

In this study, dust devils were analyzed in visible Landsat 8 image data to constrain their seasonal and size-frequency distribution and density. We compared the results with dust devil seasonal distributions and densities from Amazonis Planitia (Mars) which is known as the

region on Mars with the perhaps highest dust devil density [e.g., 2, 5–7]. In addition, several larger terrestrial dust devils are resolved in thermal Landsat 8 images. Brightness temperatures of these dust devils were compared with dust devil brightness temperatures in Amazonis Planitia obtained from the Thermal Emission Imaging System – Infrared (THEMIS-IR).

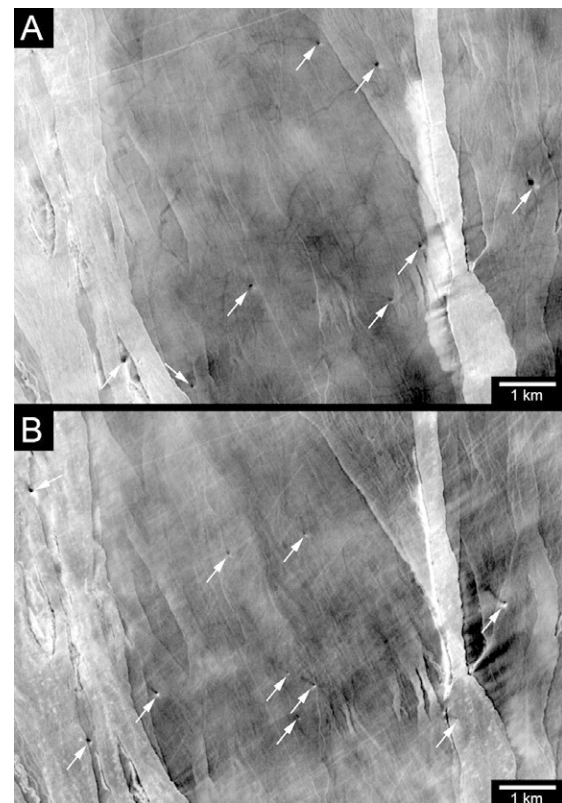


Fig. 2. (A) Landsat 8 image from 2013-05-31 showing several active dust devils and dark dust devil tracks. (B) Detail of Landsat 8 image (same region as in A) from 2013-09-04 showing several active dust devils and bright dust devil tracks. Note: Not all bright lineations are bright dust devil tracks, some are car tracks.

Data and Methods: Landsat 8 panchromatic (0.50 - 0.68 μm) image data with a spatial resolution of 15 m/pxl acquired from April 2013 to March 2014 were analyzed. In total, 40 images cover the whole or large parts of the study area (~1900 or 1500 km^2 , respectively). Image data was classified due to cloud coverage, dust haze and contrast into four quality classes (1 = high to 4 = unusable). 11 images were unusable. The number and diameter of dust devils were measured in each Landsat scene. Brightness temperatures were derived using standard procedures from Landsat Thermal Infrared data (11.50 - 12.50 μm) with a spatial resolution of 100 m/pxl. For comparison of

these results with Mars, THEMIS-VIS (0.654 μm) and IR (12.57 μm) data with spatial resolutions of 19 m/pxl and 100 m/pxl, respectively, were used.

Results: In total, 694 dust devils in 29 Landsat 8 images were identified and measured.

Seasonal distribution and density. Dust devils occurred between mid March until end of September (Fig. 3A). Dust devil activity during spring and summer is primarily expected due to their formation caused by heating of near-surface air by insolation. In Amazonis Planitia on Mars, dust devils are also predominantly active during spring and summer [2, 6, 7] (Fig. 3B). More surprisingly is the high terrestrial dust devil density with around 30–40 (max. 100) dust devils per $\text{km}^2 \times 10^3$ in comparison to Amazonis Planitia which is around 6–8 (max. 13) dust devils per $\text{km}^2 \times 10^3$ (Fig. 3). The Landsat 8 images are acquired around 10:00 local time, whereas the Amazonis Planitia analysis of [7] (Fig. 2B) is based on CTX images acquired around 15:00 local time. Based on diurnal observations on Earth [8] and Mars [9] dust devil occurrences are lower around 10:00 as around 15:00 local time, hence the differences in image acquisition times does not cause the observed higher terrestrial dust devil density. In addition, the spatial image resolution of CTX is three times higher as Landsat, hence smaller dust devils should be resolved which would increase the dust devil density. However, this is not the case indicating that the dust devil activity in the terrestrial study region is unusual high.

Size-frequency distribution. The measured terrestrial dust devils range from ~20 – 155 m in diameter. However, due to the relatively low spatial image resolution, dust devil surrounding dust clouds, and tilted dust devils towards wind direction, diameter measurements are difficult. The diameter of the dust devils were measured between the dust cloud and shadow (shadow width) which minimizes the uncertainties. We expect the error in measuring the exact diameter to be 50 % as it was also estimated for martian measurements using orbital data [3, 5]. Fig. 3C shows a size-frequency plot for the terrestrial dust devil measurements, which follows approx. a -2 power law [10]. Diameter measurements of martian dust devils in CTX images based on [7] are currently in progress.

Dust devil tracks. Dark and bright dust devil were observed to occur seasonally (Fig. 1B and 2). They are morphologically similar to dark and bright dust devil tracks investigated in situ in the regionally close Turpan desert (China) [11, 12] and might suggest an equal formation mechanism.

Thermal infrared observations. Brightness temperatures of the terrestrial dust devil cloud are about 4–5 K lower compared to the surrounding areas (Fig. 4AB). In Amazonis Planitia on Mars, brightness temperature differences are about 1 K in agreement with other studies [e.g., 4].

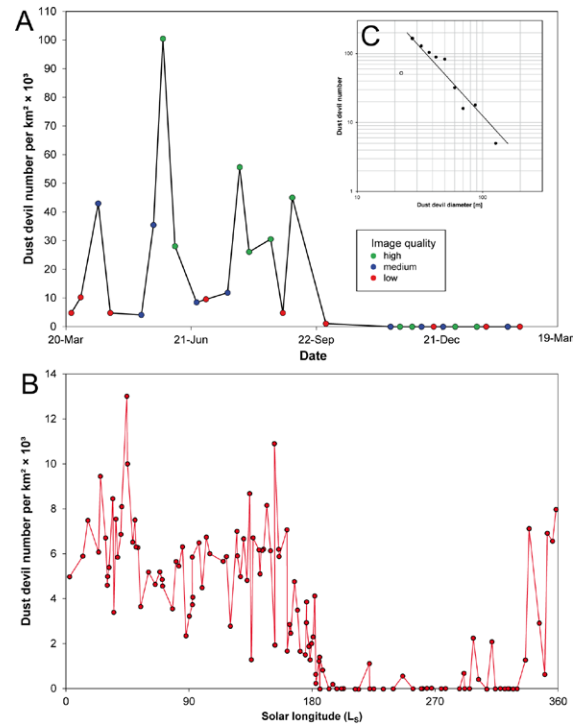


Fig. 3. (A) Seasonal dust devil density in the terrestrial study area. (B) Seasonal dust devil density in Amazonis Planitia based and modified after [7]. (C) Size-frequency plot of the measured terrestrial dust devils. Fit-by-eye line shows a -2 power law.

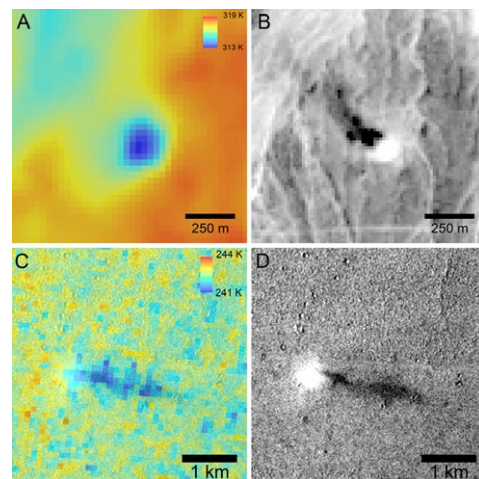


Fig. 4. (A) Brightness temperature image of a terrestrial dust devil. (B) Corresponding panchromatic image to A. (C) Brightness temperature THEMIS-IR image (I36983022) of a martian dust devil in Amazonis Planitia. (D) Corresponding panchromatic THEMIS-VIS (V36983023) image to C.

References: [1] Thomas, P. and Gierasch, P.J. (1985). *Science*, 230, 175–177. [2] Cantor, B.A. et al. (2006) *JGR*, 111, E12002. [3] Stanzel, C. (2008) *Icarus*, 197, 39–51. [4] Towner, M.C. (2009) *JGR*, 114, E02010. [5] Reiss, D. et al. (2014) *Icarus*, 227, 8–20. [6] Fisher, J.A. et al. (2005) *JGR*, 110, E03004. [7] Fenton, L.K. and Lorenz, R. (2015) *Icarus*, 260, 246–262. [8] Sinclair, P.C. (1969) *J. Appl. Meteorol.*, 8, 32–45. [9] Greeley, R. et al. (2010) *JGR*, 115, E00F02. [10] Lorenz, R.D. (2009) *Icarus*, 203, 683–684. [11] Reiss, D. (2010) *GRL*, 37, L14203. [12] Reiss, D. (2011). *Icarus*, 211, 917–920.